BIOCHEMISTRY

Kinetics of CXCL12 binding to atypical chemokine receptor 3 reveal a role for the receptor N terminus in chemokine binding

Martin Gustavsson*, Douglas P. Dyer†, Chunxia Zhao, Tracy M. Handel‡

Chemokines bind to membrane-spanning chemokine receptors, which signal through G proteins and promote cell migration. However, atypical chemokine receptor 3 (ACKR3) does not appear to couple to G proteins, and instead of directly promoting cell migration, it regulates the extracellular concentration of chemokines that it shares with the G protein–coupled receptors (GPCRs) CXCR3 and CXCR4, thereby influencing the responses of these receptors. Understanding how these receptors bind their ligands is important for understanding these different processes. Here, we applied association and dissociation kinetic measurements coupled to β-arrestin recruitment assays to investigate ACKR3:chemokine interactions. Our results showed that CXCL12 binding is unusually slow and driven by the interplay between multiple binding epitopes. We also found that the amino terminus of the receptor played a key role in chemokine binding and activation by preventing chemokine dissociation. It was thought that chemokines initially bind receptors through interactions between the globular domain of the chemokine and the receptor amino terminus, which then guides the chemokine amino terminus into the transmembrane pocket of the receptor to initiate signaling. On the basis of our kinetic data, we propose an alternative mechanism in which the amino terminus of the chemokine initially forms interactions with the extracellular loops and transmembrane pocket of the receptor, which is followed by the receptor amino terminus wrapping around the core of the chemokine to prolong its residence time. These data provide insight into how ACKR3 competes and cooperates with canonical GPCRs in its function as a scavenger receptor.

INTRODUCTION

Chemokines regulate cell migration and other physiological processes by binding to and activating chemokine receptors in the cell membrane (*1*, *2*). For most of the 20 human chemokine receptors, chemokine binding leads to G protein–mediated activation of downstream signaling pathways. Phosphorylation by G protein receptor kinases and recruitment of β-arrestins often follow and trigger additional signaling pathways as well as receptor desensitization and internalization. However, some chemokine receptors do not signal through G proteins and are therefore referred to as atypical chemokine receptors (ACKRs) (*3*). ACKR3 (also known as CXCR7), is one such ACKR that interacts with CXCL11 and CXCL12, chemokines shared by the G protein–coupled receptors (GPCRs) CXCR4 and CXCR3, respectively (*4*, *5*). In contrast to most canonical chemokine receptors that promote cell migration, one of the main functions of ACKR3 is to regulate extracellular chemokine concentrations by ligand scavenging, which, in turn, maintains responsiveness of cells expressing CXCR4 (*6*, *7*). Despite its unique pharmacology, ACKR3 appears structurally similar to the canonical G protein–coupled chemokine receptors (*8*); thus, it is unclear how it competes with CXCR4 and CXCR3 for their mutual ligands.

Similar to other class A GPCRs, the three-dimensional structure of chemokine receptors consists of seven transmembrane (7TM) helices, flanked by an extended extracellular N terminus and intracellular C terminus and connected by extracellular and intracellular loops (*9*–*12*). Chemokines are small soluble proteins composed of a disordered N terminus appended to a globular core that is stabilized by disulfide bonds. The interaction interface between chemokines and their receptors has historically been described in terms of two chemokine recognition sites (CRSs) (*2*, *13*–*15*): CRS1 includes interactions between the core of the chemokine and the N terminus of the receptor, whereas CRS2 involves the orthosteric pocket and extracellular loops of the receptor and the N terminus of the chemokine (Fig. 1A) (*16*). Crystal structures of CXCR4 in complex with the viral chemokine viral macrophage inflammatory protein–II (*17*), US28 in complex with CX3CL1 (*18*), and CCR5 in complex with an antagonist version of CCL5 (*19*) confirmed this model but also showed that chemokines have a continuous interaction interface with the receptor in the region between CRS1 and CRS2, which was consequently termed CRS1.5 (*16*, *17*). However, the crystal structures all lack information about the distal N terminus of the receptor because this region was not resolved in any of the structures. Using radiolytic footprinting experiments to define features of the ACKR3:CXCL12 complex, we recently uncovered an additional point of contact between this region (residues 2 to 7 of ACKR3) and the β1 strand of CXCL12 (*8*), and in analogy with previous nomenclature, this region is referred to as CRS0.5 (Fig. 1A). Mutagenesis studies in combination with binding and functional assays suggest that the receptor N terminus contributes primarily to chemokine binding, whereas CRS2 interactions in the receptor binding pocket are important for both binding affinity and receptor activation (*2*, *13*). Nuclear magnetic resonance studies show that soluble peptides corresponding to receptor N termini are able to interact with chemokines (*20*) and that in the case of CXCR4, the chemokine can remain bound to the full-length receptor even in the presence of a small molecule in

Skaggs School of Pharmacy and Pharmaceutical Sciences, University of California, San Diego, 9500 Gilman Drive, La Jolla, CA 92093-0684, USA.
*Present address: Department of Biomedical Sciences, University of Copenhagen, Blegdamsvej 3, 2200 Copenhagen, Denmark.
†Present address: Wellcome Centre for Cell-Matrix Research and Lydia Becker Institute of Immunology and Inflammation, Faculty of Biology, Medicine and Health, Manchester Academic Health Science Centre, University of Manchester, Manchester M13 9PT, UK.
‡Corresponding author. Email: thandel@ucsd.edu

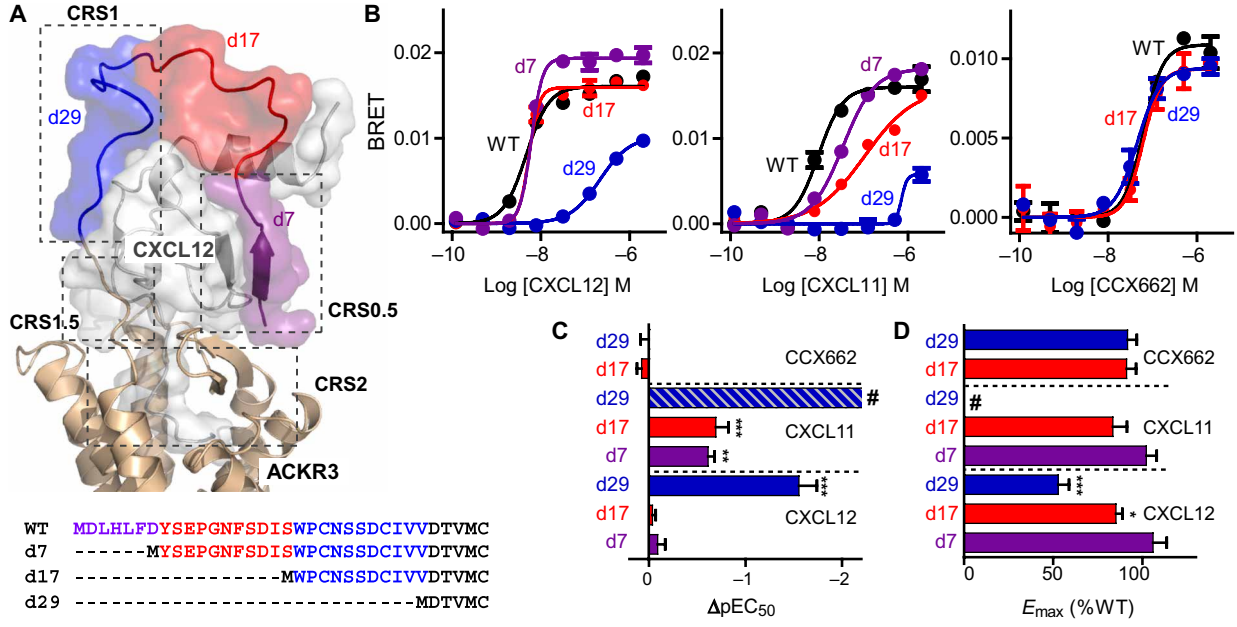

Fig. 1. Arrestin recruitment of N-terminally truncated ACKR3 variants. (**A**) Extracellular portion of the ACKR3:CXCL12 complex from experimentally driven molecular model (*8*) and sequences of ACKR3 truncation mutants. Truncated regions are highlighted according to the color scheme in the model. (**B**) Representative examples of recruitment of GFP10–β-arrestin–2 to ACKR3-Rluc3 variants stimulated with different concentrations of $CXCL12_{WT}$, CXCL11, and CCX662 measured by BRET. Each point corresponds to the average and SE of two measurements. (**C** and **D**) Potency (C) and efficacy (D) of ligand-induced β-arrestin–2 recruitment determined relative to $ACKR3_{WT}$ from fitting of dose-response curves. pEC_{50} and E_{max} values for truncation mutants were determined as $\Delta pEC_{50} = pEC_{50,mutant} - pEC_{50,WT}$ and $\%E_{max} = E_{max,mutant}/E_{max,WT} \times 100$. Data are mean and SE of three or more experiments. Significantly lowered potency or efficacy relative to $ACKR3_{WT}$ with the same ligand is noted: $^{*}P < 0.05$, $^{**}P < 0.01$, and $^{***}P < 0.001$ from one-way analysis of variance (ANOVA) with Dunnett's multiple comparison test. Pound sign (#) in (C) indicates that CXCL11-induced arrestin recruitment by $ACKR3_{d29}$ could not be accurately fit, and ΔpEC50 was estimated from the raw data to be >−2.2.

the orthosteric pocket (*21*). On the basis, in part, of these observations, the receptor's N terminus has been hypothesized to act as an initial interface for chemokine docking, which anchors the chemokine and allows the chemokine's N terminus to form interactions within the orthosteric pocket of the receptor in a two-step mechanism (*13*, *14*, *21*). However, there are little experimental data that support or refute this model, especially regarding the order in which interactions are formed and their relative importance for chemokine association and dissociation. More generally, the role that the receptor N terminus plays in chemokine binding and how interactions involving the receptor N terminus influence those in the receptor binding pocket remain to be fully elucidated.

Here, we characterized the contribution of the N terminus of ACKR3 to its binding and activation by using receptor truncations, chemokine mutants, and ligand association/dissociation kinetic experiments. The data suggest a modified mechanism for the role of the receptor N terminus in chemokine binding that differs from the previously hypothesized mechanism. Although there are no "hotspots" of interaction in the N terminus, it plays an important role in modulating the residence time of the chemokine on the receptor. The data also suggest an interdependency of interactions involving the receptor N terminus with those in the receptor binding pocket and that at least in the case of ACKR3:CXCL12, the chemokine first engages the orthosteric pocket, which is followed by interactions with the receptor N terminus. The kinetic mechanisms by which ACKR3 binds CXCL12 show key differences from CXCR4:CXCL12 that can be reconciled with its function as a scavenger receptor.

RESULTS

Truncation of the receptor N terminus affected its activation by chemokine but not by a small-molecule agonist

To test the contribution of the ACKR3 N terminus to chemokine binding and activation, we generated three N-terminal truncation mutants of ACKR3. Truncation of the first 29 residues ($ACKR3_{d29}$) removed both CRS1 and CRS0.5 regions as well as the disulfide between residue 21 and 26 (*8*); truncation of the first 17 residues ($ACKR3_{d17}$) removed CRS0.5 and part of the CRS1 region, and truncation of the first seven residues ($ACKR3_{d7}$) retained all interactions except those in the CRS0.5 region (Fig. 1A). To determine the effect of the truncations on receptor function, we then tested the ability of the mutant receptors expressed in human embryonic kidney (HEK) 293T cells with *Renilla* luciferase 3 (Rluc3) fused to their C termini to recruit green fluorescence protein 10 (GFP10)–β-arrestin–2 using a bioluminescence resonance energy transfer (BRET)–based assay. Stimulation with $CXCL12_{WT}$, $ACKR3_{d7}$, and $ACKR3_{d17}$ recruited arrestin with the same potency as $ACKR3_{WT}$ and only a slightly lowered efficacy (Fig. 1, B to D). By contrast, truncation of the first 29 residues of ACKR3 leads to a significantly lowered potency and efficacy of CXCL12-induced arrestin recruitment, indicating that the N terminus, specifically the region between residues 17 and 29, was important for receptor function.

CXCL11 showed important differences from CXCL12: Its ability to activate ACKR3 was affected by all three truncated receptor variants (Fig. 1, B to D). $ACKR3_{d7}$ and $ACKR3_{d17}$ had a significantly lowered potency compared to the wild-type receptor for CXCL11-induced β-arrestin–2 recruitment, whereas $ACKR3_{d29}$ was severely impaired and only recruited β-arrestin–2 at the highest concentration of CXCL11,

precluding an accurate determination of potency and efficacy values. These data underscore the strong dependence of CXCL11 on the ACKR3 N terminus for receptor activation.

By contrast to the chemokines, the small-molecule CCX662 (*22*), predicted to bind in the orthosteric pocket, recruited β-arrestin–2 with similar potencies and efficacies by activating $ACKR3_{WT}$, $ACKR3_{d17}$, and $ACKR3_{d29}$ (Fig. 1, B to D). Furthermore, the efficacies approached that observed for activation of $ACKR3_{WT}$ by $CXCL12_{WT}$ (fig. S1, A and B). This result confirmed that the receptor can be activated almost fully even in the absence of the N terminus and by a small-molecule agonist. It also suggested that all three ACKR3 variants are equally expressed at the surface, although this could not be directly tested because of a lack of antibodies against $ACKR3_{d17}$ and $ACKR3_{d29}$ and the need to keep the receptor N terminus free from affinity tags (fig. S2, A to D).

Together, these results showed that both CXCL11 and CXCL12 relied on interactions with the receptor N terminus for their function. The key interactions with CXCL12 appeared to involve residues 17 to 29, whereas CXCL11 required the full N terminus of the receptor (Fig. 1, B to D).

The kinetics of CXCL12 binding to ACKR3 was unusually slow

To further probe the role of the ACKR3 N terminus on its interaction with chemokine, we characterized the binding of CXCL11 and CXCL12 to $ACKR3_{WT}$ and the truncation mutants $ACKR3_{d17}$ and $ACKR3_{d29}$. Ligand binding to chemokine receptors is typically measured using equilibrium experiments to obtain median inhibitory concentration (IC_{50}) or, in some cases, dissociation constant (K_d) values. Although informative, these numbers do not provide information on association and dissociation rates of ligands, which are important for a complete understanding of the binding mechanisms and the effects of mutations. We therefore sought to develop assays to determine association and dissociation rates for chemokine binding to receptors.

Chemokine off-rates were measured by coexpressing $ACKR3_{WT}$ with hemagglutinin (HA)–tagged chemokines expressed in *Spodoptera frugiperda Sf9* cells. The chemokines were then labeled with fluorescein isothiocyanate (FITC)–conjugated antibody against HA, and after the addition of a large excess of the small-molecule CCX777 (*8*, *23*) to prevent reassociation of the chemokine, time-dependent chemokine dissociation was followed by flow cytometry. $CXCL12_{WT}$ had a dissociative half-life of 102 ± 18 min (average ± SE of $n = 6$ independent measurements, represented in Fig. 2A), which is longer than what has been reported for CCR2:CCL2 (21 min) and CXCR4:CXCL12 (1.4 min) (*24*, *25*). For example, when assayed by surface plasmon resonance (SPR) (*25*), CXCL12 had about 70-fold faster off-rate from CXCR4 than that observed for ACKR3, which was greater than about 10-fold difference in affinity between the receptors typically reported from competition binding experiments (table S1). When tested in our assays, CXCL11 had a faster dissociation rate than CXCL12. Using our current experimental setup, the dissociation was too fast to accurately quantify. These results highlight another substantial difference between the two native ligands, CXCL11 and CXCL12, in their interaction with ACKR3.

To assay chemokine association, HA-tagged $CXCL12_{WT}$ was again labeled with a FITC-conjugated anti-HA antibody. FITC-labeled $CXCL12_{WT}$ was then added to $ACKR3_{WT}$-expressing *Sf9* cells, and association was followed using flow cytometry (fig. S3A). Fitting of the association data required a multiple-component exponential due to an initial fast phase corresponding to 35 ± 4% that was too rapid to quantify using the current methods (fig. S3B). This fast phase was followed by a slower phase representing the remaining 65% of the data, which was characterized by an observed rate (k_{obs}) of 0.019 ± 0.004 min^{-1} when 10 nM $CXCL12_{WT}$ was used in the experiment (Fig. 2B). On the basis of the measured off-rate and the expression for k_{obs} of a ligand interaction with a single-state receptor, this equated to an on-rate of $1.8 \pm 0.7 \times 10^4$ M^{-1} s^{-1}, which is about 25-fold slower than what has been measured for CXCR4 (*25*).

In standard bimolecular binding reactions, k_{obs} is expected to increase linearly with increasing ligand concentration. From the association data (Fig. 2C), it is not clear whether $CXCL12_{WT}$ binding follows this ideal behavior because the cell-based experiments did not allow for a sufficiently wide range of chemokine concentrations to test this due to high receptor-independent binding of chemokines to cells at CXCL12 concentrations above 10 nM [likely because of interactions with glycosaminoglycans (*26*)]. To determine whether the binding constants were indicative of a pseudo first-order interaction and to confirm the slow kinetics of CXCL12 binding, we therefore used SPR. C-terminally biotinylated CXCL12 (CXCL12-biotin) was immobilized on an SPR chip, and the binding of purified ACKR3 reconstituted into nanodiscs (*27*) was followed at different concentrations of receptor (Fig. 2D). Fitting of the binding kinetics suggested that the SPR data followed a pseudo first-order kinetic model with a single exponential being sufficient to fit the association (fig. S4A). Association of ACKR3 to CXCL12-biotin occurred on a time scale similar to the dominant association phase seen in cells (Fig. 2E), whereas dissociation of ACKR3 in nanodiscs was faster than that detected by the cell-based methods (Fig. 2F). The faster dissociation rate was likely an effect of biotin interfering with CXCL12 binding to receptor as previously observed for S6-tagged CXCL12 binding to CXCR4 (*28*). Consistent with this hypothesis, the midpoints of thermal unfolding (T_m) of the purified ACKR3:CXCL12-biotin complex were reduced relative to ACKR3:CXCL12 (fig. S4B). Equivalent SPR experiments with ACKR3 reconstituted into *n*-dodecyl-β-D-maltopyranoside (DDM)/cholesteryl hemisuccinate (CHS) detergent micelles showed no differences in association or dissociation constants compared to the results in nanodiscs (fig. S4, C to E).

A single exponential function was sufficient to fit receptor:chemokine association in the SPR experiments, whereas association in *Sf9* cells fit best to a two-component model. A plausible reason for this difference could be the fact that receptors in cell membranes exist in different environments, which may affect chemokine association rates. The presence of cell surface glycosaminoglycans, which are well known to bind chemokines (*26*), may also contribute to apparent inhomogeneity. In addition, 7TM receptors are known to be inherently dynamic and, even in the absence of ligand, populate multiple active and inactive states (*29*), which can have different ligand association rates (*30*) and could contribute to the two-phase behavior of CXCL12 binding to ACKR3 in *Sf9* cells. This effect might be less prominent in the SPR experiments because these experiments are done at higher concentrations and with purified receptors in solution binding to immobilized chemokines, in contrast to the experiments in *Sf9* cells where soluble chemokines bind receptors immobilized in the cell membrane. A two-phase behavior similar to that observed for CXCL12 binding to ACKR3 in *Sf9* cells has been observed for live-cell ligand binding to the peptide-binding class B GPCR, parathyroid hormone 1 receptor (PTH1R), in mammalian cells (*31*). In the case of PTH1R, this behavior was explained by an initial binding step followed by a conformational rearrangement of the receptor:peptide complex.

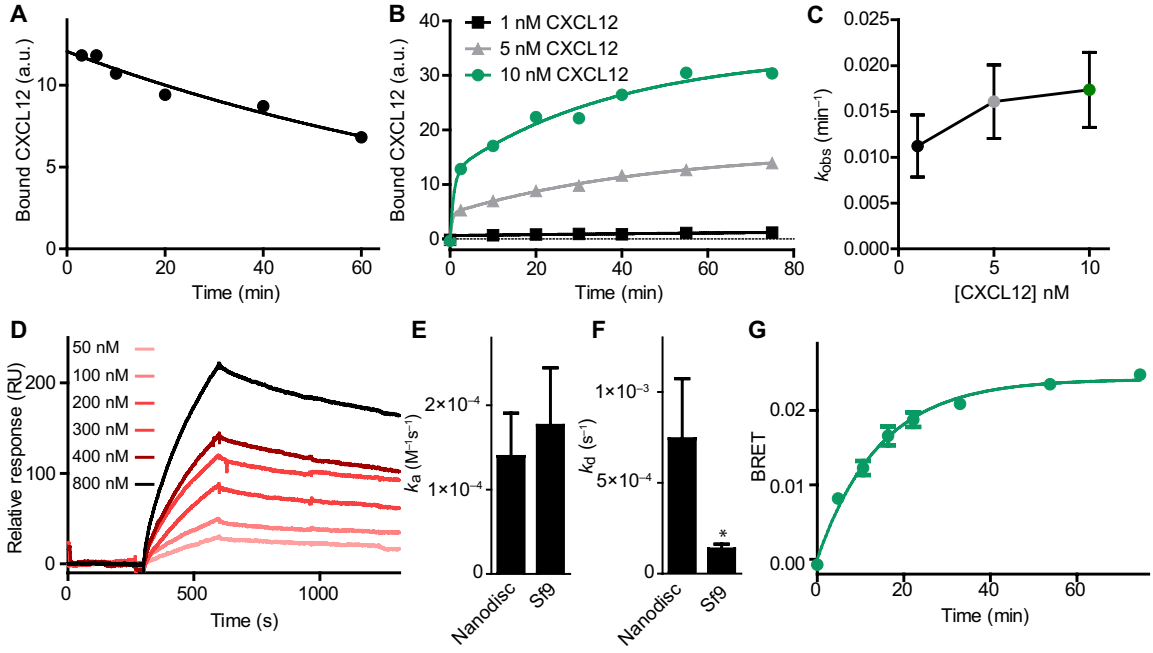

Fig. 2. Kinetics of CXCL12 binding to ACKR3. (**A**) Dissociation of $CXCL12_{WT}$ was measured by flow cytometry by monitoring the decrease in geometric mean of FITC fluorescence after addition of the small-molecule ligand CCX777 to live *Sf9* cells coexpressing $ACKR3_{WT}$ and HA-tagged $CXCL12_{WT}$ bound to FITC-conjugated antibody. a.u., arbitrary units. (**B**) Association of $CXCL12_{WT}$ to $ACKR3_{WT}$ after adding HA-tagged $CXCL12_{WT}$ complexed with FITC-conjugated antibody against HA to cells expressing $ACKR3_{WT}$. (**C**) k_{obs} values for the slow phase of $CXCL12_{WT}$ association to $ACKR3_{WT}$ at different ligand concentrations determined from fitting the data to a two-component exponential equation. (**D**) Binding of ACKR3 in nanodiscs to immobilized CXCL12 measured by SPR. RU, response units. (**E** and **F**) Association (E) and dissociation rate constants (F) were determined for binding of ACKR3 in nanodiscs to immobilized CXCL12 detected by SPR and for CXCL12 binding to ACKR3 in live *Sf9* cells detected by flow cytometry. The asterisk indicates that the dissociation rate is slower in *Sf9* cells as determined from unpaired *t* test with $P < 0.05$. **(G)** Kinetics of β-arrestin–2 recruitment to $ACKR3_{WT}$ in HEK293T cells followed by BRET. Curves in (A), (B), (D), and (G) are representative examples of six (A) or three (B, D, and G) independent results, and each point or bar in (C), (E), and (F) is means and SEs of three or more experiments.

Because our binding experiments do not distinguish different bound states, it is unlikely that a similar model explains the two-phase behavior of ACKR3.

Together, the data showed that the time scale of $CXCL12_{WT}$ binding to $ACKR3_{WT}$ was similar in three different membrane-mimicking systems (*Sf9* cells, nanodiscs, and DDM/CHS micelles), with two different experimental setups (flow cytometry and SPR) and with detection of receptor binding to immobilized chemokine or chemokine binding immobilized receptor. On the basis of these results, we concluded that the slow binding kinetics was an inherent feature of the ACKR3:CXCL12 interaction.

To further determine whether the measured binding kinetics are relevant in the context of CXCL12 activation of ACKR3, we tested the rate of arrestin association to the receptor using time-resolved BRET experiments where arrestin association was quantified at different time points after chemokine addition (Fig. 2G). When fit to a single exponential, the k_{obs} for arrestin recruitment to $ACKR3_{WT}$ induced by 10 nM $CXCL12_{WT}$ was threefold faster than the observed k_{obs} of the slow phase of binding to *Sf9* cells at the same concentration. The faster rate could be explained by the higher temperature used in the BRET experiments because HEK293T cells were maintained at 37°C during chemokine association and the *Sf9* cells and SPR experiments were performed at ambient temperature. Nevertheless, comparison of the k_{obs} values for arrestin association and CXCL12 binding showed that arrestin recruitment happened on a time scale similar to CXCL12 association, suggesting that chemokine binding could be rate limiting for arrestin association.

ACKR3 is known to have about 10-fold higher affinity for CXCL12 than CXCR4 (table S1); thus, these results suggest that hidden within this relatively modest affinity difference are more substantial differences in binding kinetics where ACKR3 has a slower CXCL12 association rate than CXCR4, but the even slower dissociation rate makes it a higher-affinity binder.

N-terminal truncations of ACKR3 affected chemokine dissociation but not association

To test the role of the receptor N terminus in ligand binding, we examined truncated versions of ACKR3 for their ability to bind ligands in stability and kinetic association/dissociation experiments. Stable expression of the truncated receptors required fusion of thermostabilized apocytochrome b562 (bril) to the N terminus of ACKR3, the addition of which did not affect the dissociation rate or fold of the receptor (fig. S5, A to D). To confirm proper folding of the truncated constructs, receptor:ligand complexes were purified from *Sf9* cells (Fig. 3A) and tested in thermostability assays (*32*). Bril-$ACKR3_{WT}$, bril-$ACKR3_{d17}$, and bril-$ACKR3_{d29}$ had identical T_m when in complex with the small-molecule CCX662 (Fig. 3B). This confirmed the structural integrity of the truncated complexes and was in perfect agreement with CCX662-induced arrestin recruitment experiments (Fig 1, B to D). In complex with the CXCL12 mutant $CXCL12_{LRHQ}$, which was selected from a phage display library (*33*) and has the first three residues in its sequence replaced by Leu-Arg-His-Gln, bril-$ACKR3_{d29}$ had a lower T_m compared to the other ACKR3 variants (Fig. 3B). This is again consistent with the data described above

(Fig. 1, B to D) where ACKR3$_{d29}$ had a lower potency and efficacy of arrestin recruitment when stimulated with CXCL12$_{WT}$. CXCL12$_{WT}$ association experiments (Fig. 3C) showed that the population of the slow receptor binding phase was slightly higher for bril-ACKR3$_{d29}$ compared to bril-ACKR3$_{WT}$ (78% versus 65%; Fig. 3D), but there was no significant difference between bril-ACKR3$_{WT}$ and bril-ACKR3$_{d17}$ or bril-ACKR3$_{d29}$ in the rate of the slow association phase (Fig. 3E). Consistent with the binding data, time-resolved BRET experiments with 10 nM CXCL12 (Fig. 3F) showed no significant differences in the rate of arrestin recruitment due to the N-terminal truncations (Fig. 3G). In contrast, bril-ACKR3$_{d29}$ had a 30-fold faster chemokine dissociation rate from receptors in *Sf9* cells compared to bril-ACKR3$_{WT}$ (Fig. 3, H and I). These data demonstrated that the main effect of the N-terminal truncation on arrestin recruitment to ACKR3$_{d29}$ can be attributed to an increased dissociation rate from the receptor. This result also suggests that the role of residues 18 to 29 of ACKR3 is primarily to prevent chemokine dissociation after the chemokine has engaged the receptor (Fig. 3J).

The impact of ACKR3 N-terminal truncation was modulated by chemokine dissociation rates

Compared to other chemokine receptors, point mutations of the ACKR3 N terminus have been reported to have relatively minor effects on the ability of the receptor to be activated by CXCL12 and CXCL11 (*34*, *35*). Our data showing that N-terminal truncations of ACKR3 had major effects on both CXCL11 and CXCL12 activation were therefore unexpected. Of the two chemokines, CXCL11-mediated β-arrestin–2 recruitment to ACKR3 was more sensitive to mutations

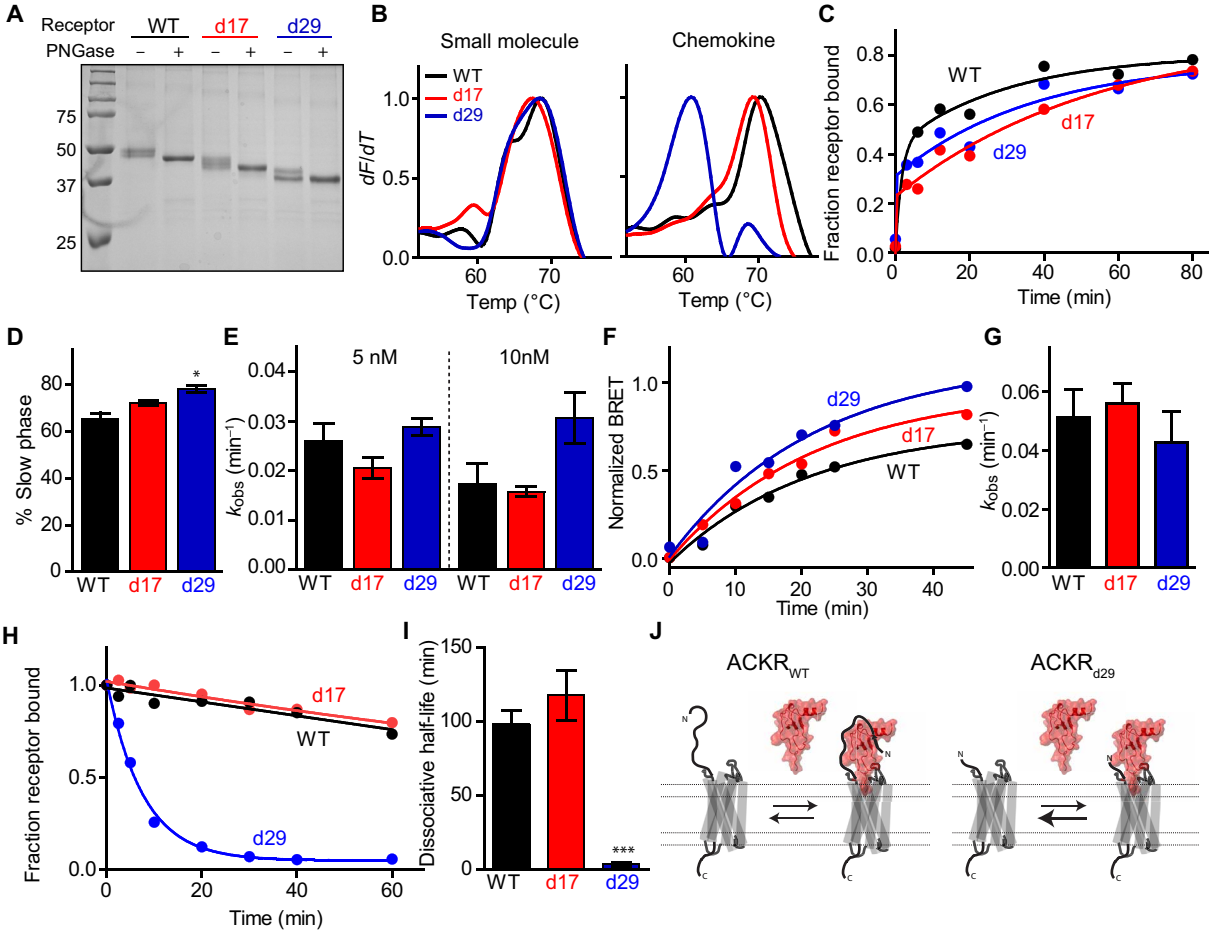

Fig. 3. Ligand binding kinetics of truncated ACKR3 variants. (**A**) Representative example of SDS-PAGE of purified bril-ACKR3$_{WT}$, bril-ACKR3$_{d17}$, and bril-ACKR3$_{d29}$. Addition of PNGase F deglycosylates the receptor. (**B**) Representative example of thermal unfolding of ACKR3 variants in complex with CCX662 and CXCL12$_{LRHQ}$ measured using CPM fluorescence (*32*). (**C**) Representative example of CXCL12$_{WT}$ association to ACKR3 variants at 5 nM chemokine detected by flow cytometry. (**D**) Percent of the association curves corresponding to the slower phase of chemokine association determined from fitting association curves at 10 nM CXCL12$_{WT}$ to a two-phase exponential equation. Bars represent the average and SEs of three or more experiments. ACKR3$_{d29}$ has a larger slow component than ACKR3$_{WT}$ (*$P < 0.05$ as determined from one-way ANOVA with Dunnett's multiple comparison test). (**E**) Mean and SEs from three or more measurements of k_{obs} values for the slow phase in (D). (**F**) Representative example of arrestin recruitment to ACKR3 variants determined from BRET experiments after addition of 10 nM CXCL12$_{WT}$. (**G**) Average and SEs of k_{obs} values from fitting three time-resolved BRET experiments to single exponential equations. (**H**) Representative example of CXCL12$_{WT}$ dissociation from ACKR3:CXCL12 complexes in *Sf9* cells. (**I**) Mean and SEs of CXCL12$_{WT}$ dissociative half-life determined from fitting three or more dissociation curves to a single-phase exponential equation. The dissociative half-life of bril-ACKR3$_{d29}$ is significantly shorter than ACKR3$_{WT}$ (***$P < 0.001$ as determined from one-way ANOVA with Dunnett's multiple comparison test). (**J**) Schematic representation of CXCL12 binding equilibria for ACKR3$_{WT}$ and ACKR3$_{d29}$ highlighting the faster dissociation rate but unchanged association rate of CXCL12 binding to the truncated receptor.

(*34*) and truncations of the receptor N terminus than recruitment induced by CXCL12 (Fig 1, B to D). In addition, CXCL11 had a faster off-rate from the receptor than CXCL12, too fast to measure with our assay. On the basis of these observations, we hypothesized that the dissociation rate of a chemokine may affect how sensitive its potency and efficacy of activation are to N-terminal receptor truncations. To test this hypothesis, we compared binding kinetics and β-arrestin recruitment of $CXCL12_{WT}$ to the single-point mutant $CXCL12_{P2G}$ (*14*) and to $CXCL12_{LRHQ}$ (*33*). These two variants only differ from $CXCL12_{WT}$ in the distal N-terminal region of the chemokine that interacts in the CRS2 region (orthosteric pocket and extracellular loops) of the receptor. Thus, the interactions that the first 29 residues of ACKR3 make with the chemokines are identical and far separated from the ACKR3:CXCL12 interactions that are unique to the respective chemokine (Fig. 4A). It has been previously shown that all three CXCL12 variants are high-affinity ligands of ACKR3 with IC_{50} values in the picomolar to low nanomolar range (*33*). However, preliminary coexpression experiments suggested different binding kinetics for the three chemokines because $CXCL12_{WT}$ and $CXCL12_{LRHQ}$ could be copurified with ACKR3 from *Sf9* cells (*27*), whereas $CXCL12_{P2G}$ could not, presumably because it rapidly dissociated from the receptor.

To quantify these potential differences, we tested the mutant chemokines with bril-$ACKR3_{WT}$ and bril-$ACKR3_{d29}$ in dissociation experiments. $CXCL12_{WT}$, $CXCL12_{P2G}$, and $CXCL12_{LRHQ}$ had significantly different off-rates from bril-$ACKR3_{WT}$ ranging from $CXCL12_{P2G}$, which had a dissociative half-life of 7.2 ± 1.2 min (~15-fold faster than $ACKR3_{WT}$), to $CXCL12_{LRHQ}$, which had no measurable dissociation during the time scale of the experiment (Fig. 4, B and C). Differences in dissociation rates were even further enhanced with the truncated receptor bril-$ACKR3_{d29}$. $CXCL12_{LRHQ}$ was fully bound even after 60 min of competition with unlabeled ligand, although we were unable to determine detectable binding of $CXCL12_{P2G}$ due to its rapid dissociation rate (Fig. 4, D and E).

Despite differences in dissociation rates from the receptor, all three chemokine mutants induced β-arrestin recruitment to $ACKR3_{WT}$ with similar efficacy and potency (Fig 4, F to H). This was consistent with the idea that the exact sequence of the chemokine N terminus is not crucial for ACKR3 activation (*35*), which contrasts with most canonical G protein–coupled chemokine receptor:chemokine pairs where specific interactions with the chemokine N terminus play a crucial role in signaling (*16*). However, significant differences in the ability to promote β-arrestin–2 recruitment to the truncated receptor $ACKR3_{d29}$ were observed for the three chemokines (Fig 4, G to I). $CXCL12_{LRHQ}$ recruited β-arrestin–2 to the truncated receptor with higher efficacy and potency than the other chemokines, including $CXCL12_{WT}$, whereas $CXCL12_{P2G}$ was a very weak agonist that was only able to recruit a small amount of β-arrestin–2 even at 2 μM chemokine (fig. S6).

Thus, the chemokine with the slowest dissociation rate was also the one least affected by the N-terminal truncation of the receptor in agreement with the hypothesis that there is a correlation between a fast chemokine off-rate and sensitivity to N-terminal receptor truncation and mutations. This further suggests that the residence time of agonists on ACKR3 affects their ability to recruit β-arrestin–2.

DISCUSSION

On the basis of previous studies, it has been proposed that the chemokine receptor N terminus acts as a landing pad for the core of the chemokine, which then orients the chemokine N terminus to activate the receptor through interactions in the orthosteric pocket (*13*, *14*). However, the order of binding has never been experimentally demonstrated. On the basis of our studies of CXCL12 binding to ACKR3, we propose a different model where interactions are initially formed between the N terminus of the chemokine and the orthosteric pocket and extracellular loops of the receptor (CRS1.5/CRS2 region in Fig. 1A). This initial interaction is followed by the N terminus of the receptor wrapping around the chemokine to form the CRS0.5/CRS1 interactions and anchoring the chemokine to the receptor (Fig. 5).

Our results showed that chemokine binding is driven by the interplay between different epitopes (CRS0.5/1/1.5/2) on the receptor and that the contribution from these epitopes cannot be completely uncoupled. The ACKR3 N terminus had a critical role in chemokine binding and activation. However, this role is dependent not only on the specific "CRS1" interactions but also rather on the total sum of interactions that the chemokine makes with other regions of the receptor. These observations suggest that truncations and mutations of the receptor or chemokine N termini may affect the potency and efficacy of activation by the chemokine but only if the truncated or mutated region contributes a large enough fraction of the total binding energy. CXCL11-induced ACKR3 activation was more sensitive than CXCL12-induced activation to N-terminal receptor mutations (*34*) and truncations. According to our model, CXCL11 does not necessarily make more and/or stronger interactions with the distal N terminus of the receptor, but those interactions represent a larger portion of the total interaction energy. Similarly, CXCL12 binding and activation of ACKR3 are less sensitive to point mutations in the receptor N terminus than CXCL12 binding and activation of CXCR4 (*34*, *35*). It was therefore suggested that, as opposed to CXCR4, interactions with the ACKR3 N terminus is not an essential determinant of CXCL11- and CXCL12-induced receptor activation (*35*). Our data showed that the ACKR3 N terminus plays a key role in chemokine binding and activation and suggest that the reason for ACKR3's reduced sensitivity to mutations is that CXCL12 has a much slower off-rate from ACKR3 than from CXCR4.

Biased signaling where ligands or receptor variants selectively activate one signaling pathway over another is an emerging concept (*36*). Our observations suggest a potential mechanism for how CRS0.5/1 interactions could control receptor activation of different signaling pathways. A chemokine with fast dissociation rate may not have a long enough residence time on the receptor to allow for G protein kinase phosphorylation followed by β-arrestin recruitment. Thus, changes in chemokine residence times may alter the coupling to different intracellular adaptor proteins and may be a source of apparent signaling bias. This would be analogous to the dopamine D_2 receptor where apparent signaling bias is affected by agonist dissociation rates (*37*). In this study, we used β-arrestin–2 recruitment as a measure of receptor activation. However, recent studies have shown differences in intracellular trafficking between CXCL11- and CXCL12-activated ACKR3, potentially because of interaction with other adaptor proteins than arrestins (*38*). In this case and in the case of other receptors, intracellular effector proteins may be differentially affected by changes in ligand lifetimes on receptors.

Although our data suggest that the main contribution of the N terminus is to prevent the chemokine from dissociating from the receptor, it should also be noted that $CXCL12_{LRHQ}$ has a lower efficacy for $ACKR3_{d29}$ than for $ACKR3_{WT}$ even with its very long dissociative half-life (longer than that of $CXCL12_{WT}$ from $ACKR3_{WT}$). Thus, although $ACKR3_{d29}$ can be fully activated by a small-molecule agonist,

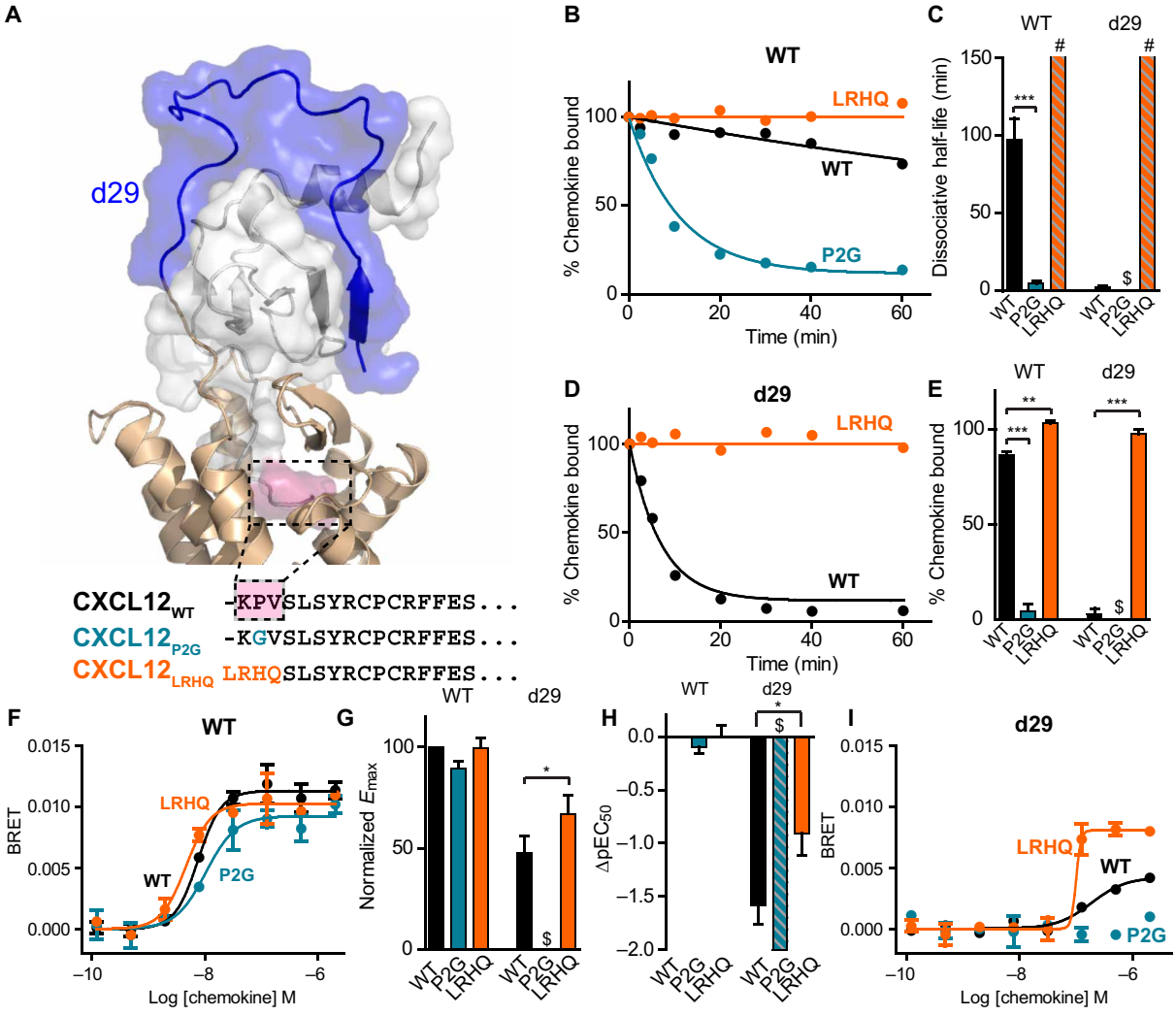

Fig. 4. ACKR3 binding kinetics and arrestin recruitment of CXCL12 mutants. (**A**) Extracellular portion of ACKR3:CXCL12 model and N-terminal sequences of CXCL12 variants. Residues in $CXCL12_{WT}$ that differ between the three mutants are highlighted in pink in the model. (**B**) Representative curves for CXCL12 dissociation from bril-$ACKR3_{WT}$ detected by flow cytometry. (**C**) Means and SEs from three or more experiments of dissociative half-lives determined from fitting dissociation curves to a single exponential. The dissociative half-life of $CXCL12_{LRHQ}$ was too slow to quantify but was estimated to be longer than 150 min (highlighted by # in the figure). Binding of $CXCL12_{P2G}$ to $ACKR3_{d29}$ was too low to quantify a dissociation rate [highlighted by the dollar sign ($) in the figure]. (**D**) Representative CXCL12 dissociation curves from bril-$ACKR3_{d29}$ detected by flow cytometry. (**E**) Means and SEs of the percent-specific chemokine binding remaining 20 min after the start of dissociation for three or more experiments. $CXCL12_{LRHQ}$ has a higher fraction of chemokine bound than $CXCL12_{WT}$ for both bril-$ACKR3_{WT}$ and bril-$ACKR3_{d29}$, and $CXCL12_{P2G}$ has a lower fraction bound for bril-$ACKR3_{WT}$. Binding of $CXCL12_{P2G}$ to $ACKR3_{d29}$ was too low to quantify (highlighted by $ in figure). (**F**) Representative dose-response curves for β-arrestin–2 recruitment to $ACKR3_{WT}$ and $ACKR3_{d29}$. **(G)** E_{max} normalized to $ACKR3_{WT}$ with $CXCL12_{WT}$ ($\%E_{max} = E_{max,mutant}/E_{max,WT} \times 100$). Each bar represents the average and SEs of three or more experiments. (**H**) Mean and SEs of pEC_{50} relative to $ACKR3_{WT}$ with $CXCL12_{WT}$ ($\Delta pEC_{50} = pEC_{50,mutant} - pEC_{50,WT}$). $CXCL12_{P2G}$-mediated recruitment of arrestin to $ACKR3_{d29}$ was barely detectable, and the ΔpEC_{50} was estimated to be less than −2 [highlighted by $ in (G) and (H)]. (**I**) Representative dose-response curves for β-arrestin–2 recruitment to $ACKR3_{WT}$ and $ACKR3_{d29}$. Significant differences for $CXCL12_{P2G}$ and $CXCL12_{LRHQ}$ compared to $CXCL12_{WT}$ are noted: $^*P < 0.05$, $^{**}P < 0.01$, and $^{***}P < 0.001$ from one-way ANOVA with Dunnett's multiple comparison test.

there must be additional interactions within the receptor:chemokine complex that are needed for full activation of the receptor and that are not formed when the chemokine binds the truncated receptor.

The results presented here are likely to also apply to other chemokines and chemokine receptors. Mutational studies have shown that chemokines rely, to different extents, on CRS2 interactions versus interactions involving the receptor N termini (CRS0.5/1/1.5) (*2*). For example, N-terminally truncated CCL2 is a high-affinity CCR2 antagonist (*39*). On the other hand, N-terminal truncations significantly affect the ability of CXCL12 to bind and activate CXCR4 (*40*). Our efforts were focused on ACKR3 and CXCL12, which comprise a CXC receptor:CXC chemokine pair and are likely not representative of the whole family of receptors and chemokines. Thus, more data with other receptors and chemokines would further clarify the role of the receptor N terminus in chemokine binding. Nonetheless, previous results have shown similarities between the ACKR3:CXCL12 complex and the same chemokine in complex with CXCR4. For example, several residues that affect CXCR4 chemokine binding and activation are also implicated in CXCL12 activation of ACKR3 (*8*, *41*).

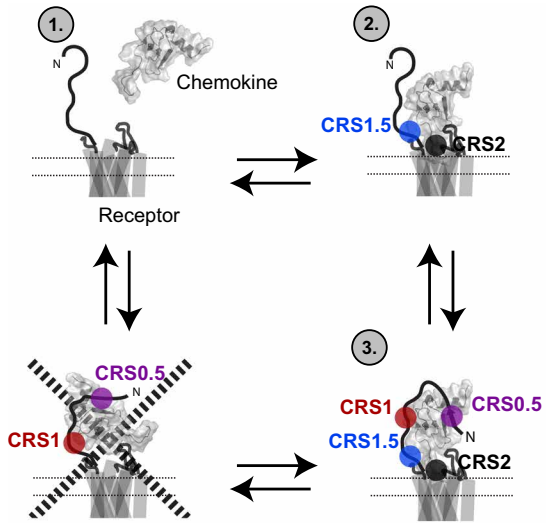

Fig. 5. Model of the mechanism of chemokine interaction with the receptor. Experiments with chemokine mutations ($CXCL12_{P2G}$ and $CXCL12_{LRHQ}$) and receptor truncations ($ACKR3_{d29}$) suggested that the chemokine initially engages with the CRS1.5 and CRS2 of the receptor followed by formation of additional interactions with the CRS0.5 and CRS1 epitopes. Initial docking of the receptor N terminus with the core of the chemokine (bottom left corner) is not a key step in the formation of the fully engaged receptor:chemokine complex.

Posttranslational modifications of the N terminus have been identified for a number of different chemokine receptors. A notable example of this is Tyr sulfation that occurs for multiple receptors (*42*) and can have major effects on chemokine binding affinity (*43*). On the basis of our model, sulfation likely reduces the dissociation rates of chemokine. In analogy with the effects of N-terminal truncation of ACKR3 on CXCL11 and CXCL12, this modification could therefore serve as a regulatory mechanism that affects signaling, with different effects on specific chemokines that bind to the same receptor.

Both association and dissociation rates of CXCL12 binding to ACKR3 are slower than what has been reported for binding to CXCR4. One of the proposed roles of ACKR3 is to regulate CXCR4 by controlling the extracellular concentration of CXCL12 (*6*, *7*). On the basis of its higher affinity for CXCL12, it was believed that the chemokine would preferentially bind ACKR3 over CXCR4 (*44*). However, although this may be observed in equilibrium experiments, the kinetic differences between the two receptors, with the CXCR4 on- and off-rates being considerably faster than those for ACKR3, could make CXCR4 kinetically favored for CXCL12 binding. In such a hypothetical scenario, CXCL12 may initially bind CXCR4, leading to G protein–coupled signaling, but eventually favor ACKR3 binding, which would lead to chemokine internalization and degradation. Thus, differences in their binding kinetics could be of fundamental importance for the interplay between ACKR3 and CXCR4 in vivo.

MATERIALS AND METHODS

Cloning

A pFastBac1 vector containing residues 2 to 332 of human ACKR3 with an N-terminal GP64 promoter, HA signal sequence, and C-terminal FLAG and 10× His tags was used for baculovirus expression (*27*). For expression in HEK293T cells, human ACKR3 was cloned into a pcDNA vector containing the *Rluc3* gene (a gift from N. Heveker, Université de Montréal, Montréal, Québec, Canada) at the C terminus of the receptor. Constructs where 7 to 29 residues were removed from the receptor N terminus were obtained using the site-directed, ligase-independent mutagenesis (SLIM) protocol (*45*). For chemokine expression in *Sf9* cells, CXCL11 and CXCL12 with their native signal sequences and C-terminal HA tags were cloned into a pFastBac1 vector containing a polyhedrin promoter. $CXCL12_{P2G}$ and $CXCL12_{LRHQ}$ mutant constructs were produced by site-directed mutagenesis using standard quick-change methods.

Ligands

Recombinant CXCL11, $CXCL12_{WT}$, $CXCL12_{P2G}$, and $CXCL12_{LRHQ}$ were expressed and purified from *Escherichia coli* by slight variations of the protocols previously described (*8*, *46*). Small-molecule ACKR3 ligands CCX662 and CCX777 were a gift from ChemoCentryx (*23*).

BRET-based β-arrestin–2 recruitment assays

HEK293T cells were maintained in Dulbecco's modified Eagle's medium supplemented with 10% fetal bovine serum. Cells were transfected in six-well plates with 0.05 to 0.125 μg of ACKR3 DNA and 1 μg of a pcDNA vector containing GFP10–β-arrestin–2 (gift from N. Heveker, Université de Montréal). Forty-eight hours after transfection, the cells were washed and resuspended in phosphate-buffered saline (PBS) buffer containing 0.1% glucose and transferred to 96-well white clear-bottom tissue culture assay plates (BD Falcon) (100,000 cells per well). For dose-response experiments, the plates were incubated for 40 min at 37°C and then stimulated for 20 min with different concentrations of ligand. β-Arrestin–2 expression was quantified by measuring GFP10 fluorescence emission at 510 nm after excitation at 400 nm. The bottom of the plate was covered, and luciferase substrate (Deep Blue C) was added to a final concentration of 5 μM. BRET was measured on a VICTOR X Light multilabel plate reader (PerkinElmer Life Sciences) as the ratio of GFP10 emission at 515 nm to Rluc3 emission at 410 nm. Each point was recorded in duplicate; average BRET values were plotted against log [ligand], and the resulting dose-response curves were fit using nonlinear fitting in GraphPad Prism to obtain maximum activity (E_{max}) and the negative logarithm of the ligand concentration at half E_{max} (pEC_{50}) values. For time-resolved BRET experiments, cells were incubated for 40 min and then stimulated with 10 nM chemokine for times ranging from 4 to 70 min before measuring BRET. Averaged BRET values from duplicate measurements were plotted as a function of time, and the association rates were determined from nonlinear fitting to single exponential functions.

Sf9 cell expression

ACKR3 was expressed in *Sf9* cells as previously described (*27*). Briefly, cells were cultured in ESF 921 media (Expression Systems) at 27°C with shaking at 140 rpm. The Bac-to-Bac Baculovirus Expression System (Invitrogen) was used to produce baculovirus containing the different ACKR3 and CXCL12 variants as previously described (*27*). Briefly, recombinant bacmids were incubated with 3 μl of X-tremeGENE Transfection Reagent (Roche) and 100 μl of transfection medium (Expression Systems) for 30 min. The mixture was added to 2.5 ml of *Sf9* cells at a density of 1.3×10^6 cells ml^{-1}, and the cells were incubated for 96 hours with 300 rpm shaking at 27°C. Cells were pelleted using centrifugation, and 400 μl of the resulting supernatant (P0 stock) was used to transfect 40 ml of *Sf9* cells at a density of 2.5×10^6 cells ml^{-1}. After 48 hours, the cells were centrifuged, and

the resulting supernatant was stored at 4°C until further use (P1 stock). Virus titers were determined using flow cytometry staining with a phycoerythrin-conjugated GP64 antibody. To initiate protein expression, P1 virus corresponding to ACKR3 alone or ACKR3 and CXCL12 (coexpression) was added to Sf9 cells at a density of ~2.5×10^6 cells ml^{-1} at a multiplicity of infection of 5. Cells were grown for 48 hours at 27°C with shaking at 140 rpm before experiments.

Binding experiments

For association experiments, Sf9 cells expressing ACKR3 were washed twice in assay buffer (20 mM PBS and 0.5% bovine serum albumin) and resuspended to a density of 3×10^6 cells ml^{-1}. Ten microliters (30,000 cells) of cells was transferred to a 96-well assay plate, and 2 μl from the viability dye 7-amino-actinomycin D (7AAD; 0.05 mg ml^{-1}), and 68 μl of room temperature assay buffer were added to each well. Purified HA-tagged $CXCL12_{WT}$ was incubated with a 1.3-fold molar excess of FITC-conjugated anti-HA antibody (Sigma-Aldrich, H7411) for 20 min. The CXCL12:antibody stock was then combined with assay buffer to make 5, 25, and 50 nM (5×) solutions, which were added to a final concentration of 1, 5, or 10 nM in a final volume of 100 μl. To quantify nonspecific binding of $CXCL12_{WT}$, the small-molecule ligand CCX777 (20 μM) was added to cells before addition of chemokine. Cells were fixed at different time points with a 0.67% (w/v) final concentration of paraformaldehyde.

For dissociation experiments, 10 μl of *Sf9* cells (30,000 cells) coexpressing ACKR3 and HA-tagged chemokine were incubated with FITC-conjugated anti-HA antibody [final antibody dilution, 200× from stock (1 mg ml^{-1})] and 1 μl of 7AAD solution [from stock (0.05 mg ml^{-1})]. After 20 min of incubation, assay buffer containing 20 μM CCX777 was added, and cells were fixed at different time points with 0.67% (w/v) of paraformaldehyde. Nonspecific binding was measured by expressing respective HA-tagged chemokine in the absence of ACKR3. Total receptor expression was measured by incubating 10 μl of cells with FITC-conjugated anti-FLAG antibody and 0.0075% (v/v) Triton X-100 and acquiring FITC fluorescence. Chemokine binding was quantified from FITC fluorescence using a Guava easyCyte flow cytometer (Millipore). Data were analyzed using FlowJo. The geometric mean of FITC fluorescence for live cells (selected from 7AAD fluorescence) was plotted against time, and nonspecific binding was subtracted. The resulting specific binding was fit using exponential functions in GraphPad Prism.

Thermostability assays

ACKR3 was purified from *Sf9* membranes as previously described (*8*, *27*). Briefly, pellets corresponding to 40 ml of *Sf9* cells expressing different ACKR3 variants (bril-$ACKR3_{WT}$, bril-$ACKR3_{d17}$, and bril-$ACKR3_{d29}$) were thawed and washed with low- and high-salt buffers [10 mM Hepes (pH 7.5), 10 mM $MgCl_2$, 20 mM KCl, and 0 or 1 M NaCl]. Washed membranes were solubilized with buffer containing 50 mM Hepes (pH 7.5), 400 mM NaCl, 0.75/0.15% (w/v) DDM/CHS, and 50 μM CCX777, and receptor was purified by affinity chromatography using TALON IMAC resin (Teknova). Eluted protein was buffer exchanged into 50 mM Hepes (pH 7.5), 10% glycerol, 150 mM NaCl, and 0.025/0.005% (w/v) DDM/CHS (exchange buffer) and stored at 4°C for up to 2 weeks. Receptor glycosylation was removed by incubation over night with PNGase F (New England BioLabs). For SDS–polyacrylamide gel electrophoresis (SDS-PAGE) analysis, ~6 μg of receptor was incubated with SDS-PAGE sample buffer and separated on 10% tris-tricine polyacrylamide gels. For thermostability assays, 0.3 μM ACKR3 and 2.5 μM 7-diethylamino-3-(40-maleimidylphenyl)-4-methylcoumarin (CPM) were incubated for 15 min in exchange buffer. Thermostability was determined using a Rotor-Gene Q 6plex reverse transcription polymerase chain reaction instrument (QIAGEN) from the increase in CPM fluorescence (excitation, 365 nm and emission, 460 nm) when the sample temperature was ramped from 25° to 95°C.

Surface plasmon resonance

SPR experiments were performed on a BIAcore 3000 machine (GE Healthcare) using a CM5 chip (GE Healthcare) and a method adapted from Dyer *et al.* (*26*). After equilibration with running buffer [10 mM Hepes, 150 mM NaCl, and 3 mM EDTA (pH 7.4)], two flow cells on the CM5 chip were activated with a 1:1 mix of 0.1 M 1-ethyl-3-(3-dimethylaminopropyl)carbodiimide and 0.2 M *N*-hydroxysuccinimide (300 μl in total). NeutrAvidin (Invitrogen) was then flowed over the activated surface [0.2 mg ml^{-1} in 20 mM sodium acetate (pH 6.0)] until surface saturation was reached, followed by surface deactivation with ethanolamine. Both flow cells were then thoroughly washed to remove nonbound NeutrAvidin using regeneration buffer [0.1 M glycine, 1 M NaCl, and 0.1% Tween 20 (pH 9.5)]. Biotinylated CXCL12 (*46*) was then flowed over one flow cell of the chip at 10 μl min^{-1} [10 μg ml^{-1} in 10 mM Hepes and 150 mM NaCl (pH 7.4)] until surface saturation was reached followed by washing with regeneration buffer. A paired flow cell with NeutrAvidin, but without CXCL12, was prepared at the same time for reference subtraction to analyze specific interactions with immobilized CXCL12.

ACKR3 purified in DDM/CHS (see the "Thermostability assays" section for details) was reconstituted into membrane scaffolding protein (MSP) 1E3D1 nanodiscs as described previously (*27*). Briefly, receptor was mixed in cholate buffer [25 mM Hepes (pH 7.5), 150 mM NaCl, 25 mM sodium cholate] with MSP1E3D1 protein and 1-palmitoyl-2-oleoyl-sn-glycero-3-phosphocholine/1-palmitoyl-2-oleoyl-sn-glycero-3-phospho-(1′-rac-glycerol) (POPC/POPG, molar ratio 3:2) lipids at a 0.1:1:110 molar ratio of ACKR3:MSP:lipid. Cholate was removed using biobeads, and nanodiscs were purified by size exclusion chromatography. Protein-containing nanodiscs were separated from empty nanodiscs by binding to TALON resin and eluted by 250 mM imidazole. The final sample was obtained after buffer exchange into 25 mM Hepes (pH 7.5) and 150 mM NaCl using spin concentrators.

Pilot experiments showed that flow rate had no effect upon the interaction or associated residual plots. Experiments were undertaken at a fast flow rate of 40 μl min^{-1}, thus ensuring that there were limited mass transfer–mediated effects in these experiments. Pilot experiments demonstrated that the regeneration buffer used removed all of the bound material and had no effect on subsequent interaction analyses.

Interaction experiments were undertaken by flowing the indicated concentrations of ACKR3 [in 10 mM Hepes, 150 mM NaCl, and 3 mM EDTA (pH 7.4) for nanodisc samples, same buffer containing 0.025/0.005% (w/v) DDM/CHS for experiments in micelles] over both flow cells with the nonspecific interaction signal (no CXCL12) being subtracted from the specific interaction signal (with CXCL12). Because of subtle mismatches between the assay buffer and the ACKR3-containing buffer, the curves produced by injecting ACKR3 buffer alone were also subtracted from the raw data. The surface was regenerated between ACKR3 injections using regeneration buffer. To ensure that the signal produced was from ACKR3 specifically, receptor-free nanodiscs were also flowed over the surface at matching concentrations, producing no positive signal.

Curves generated as above were then analyzed using the BIA evaluation software (GE Healthcare) using a 1:1 binding model. The dissociation phase of curves measured at different ACKR3 concentrations were fit to a global dissociation constant, which was then used to fit the association phase. Initially, local association constants (k_a) for each chemokine concentrations were obtained to confirm that the binding reaction followed pseudo first-order kinetics. To obtain a single k_a value for the experiment, curves at different chemokine concentrations were then fit globally.

SUPPLEMENTARY MATERIALS

stke.sciencemag.org/cgi/content/full/12/598/eaaw3657/DC1

Fig. S1. β-Arrestin recruitment to $ACKR3_{WT}$ induced by CCX662 and CXCL11 in BRET experiments.

Fig. S2. Expression of ACKR3 variants in HEK cells.

Fig. S3. Kinetics of association of CXCL12 with ACKR3 on live *Sf9* cells.

Fig. S4. SPR in nanodiscs and detergent micelles.

Fig. S5. N-terminal cytochrome b562-RIL fusion protein did not affect CXCL12 dissociation rate or folding of ACKR3.

Fig. S6. BRET signal increase after addition of 2 μM chemokine for $ACKR3_{WT}$ and $ACKR3_{d29}$.

Table S1. IC_{50} values (nM) for equilibrium binding studies reported in literature.

References (*47*–*51*)

REFERENCES AND NOTES

1. J. W. Griffith, C. L. Sokol, A. D. Luster, Chemokines and chemokine receptors: Positioning cells for host defense and immunity. *Annu. Rev. Immunol.* **32**, 659–702 (2014).
2. S. J. Allen, S. E. Crown, T. M. Handel, Chemokine: Receptor structure, interactions, and antagonism. *Annu. Rev. Immunol.* **25**, 787–820 (2007).
3. R. J. Nibbs, G. J. Graham, Immune regulation by atypical chemokine receptors. *Nat. Rev. Immunol.* **13**, 815–829 (2013).
4. J. M. Burns, B. C. Summers, Y. Wang, A. Melikian, R. Berahovich, Z. Miao, M. E. Penfold, M. J. Sunshine, D. R. Littman, C. J. Kuo, K. Wei, B. E. McMaster, K. Wright, M. C. Howard, T. J. Schall, A novel chemokine receptor for SDF-1 and I-TAC involved in cell survival, cell adhesion, and tumor development. *J. Exp. Med.* **203**, 2201–2213 (2006).
5. S. Rajagopal, J. Kim, S. Ahn, S. Craig, C. M. Lam, N. P. Gerard, C. Gerard, R. J. Lefkowitz, β-arrestin- but not G protein-mediated signaling by the "decoy" receptor CXCR7. *Proc. Natl. Acad. Sci. U.S.A.* **107**, 628–632 (2010).
6. K. E. Luker, S. A. Lewin, L. A. Mihalko, B. T. Schmidt, J. S. Winkler, N. L. Coggins, D. G. Thomas, G. D. Luker, Scavenging of CXCL12 by CXCR7 promotes tumor growth and metastasis of CXCR4-positive breast cancer cells. *Oncogene* **31**, 4750–4758 (2012).
7. P. Abe, W. Mueller, D. Schütz, F. MacKay, M. Thelen, P. Zhang, R. Stumm, CXCR7 prevents excessive CXCL12-mediated downregulation of CXCR4 in migrating cortical interneurons. *Development* **141**, 1857–1863 (2014).
8. M. Gustavsson, L. Wang, N. van Gils, B. S. Stephens, P. Zhang, T. J. Schall, S. Yang, R. Abagyan, M. R. Chance, I. Kufareva, T. M. Handel, Structural basis of ligand interaction with atypical chemokine receptor 3. *Nat. Commun.* **8**, 14135 (2017).
9. Q. Tan, Y. Zhu, J. Li, Z. Chen, G. W. Han, I. Kufareva, T. Li, L. Ma, G. Fenalti, W. Zhang, X. Xie, H. Yang, H. Jiang, V. Cherezov, H. Liu, R. C. Stevens, Q. Zhao, B. Wu, Structure of the CCR5 chemokine receptor-HIV entry inhibitor maraviroc complex. *Science* **341**, 1387–1390 (2013).
10. B. Wu, E. Y. Chien, C. D. Mol, G. Fenalti, W. Liu, V. Katritch, R. Abagyan, A. Brooun, P. Wells, F. C. Bi, D. J. Hamel, P. Kuhn, T. M. Handel, V. Cherezov, R. C. Stevens, Structures of the CXCR4 chemokine GPCR with small-molecule and cyclic peptide antagonists. *Science* **330**, 1066–1071 (2010).
11. Y. Zheng, L. Qin, N. V. Zacarías, H. de Vries, G. W. Han, M. Gustavsson, M. Dabros, C. Zhao, R. J. Cherney, P. Carter, D. Stamos, R. Abagyan, V. Cherezov, R. C. Stevens, A. P. IJzerman, L. H. Heitman, A. Tebben, I. Kufareva, T. M. Handel, Structure of CC chemokine receptor 2 with orthosteric and allosteric antagonists. *Nature* **540**, 458–461 (2016).
12. C. Oswald, M. Rappas, J. Kean, A. S. Doré, J. C. Errey, K. Bennett, F. Deflorian, J. A. Christopher, A. Jazayeri, J. S. Mason, M. Congreve, R. M. Cooke, F. H. Marshall, Intracellular allosteric antagonism of the CCR9 receptor. *Nature* **540**, 462–465 (2016).
13. D. J. Scholten, M. Canals, D. Maussang, L. Roumen, M. J. Smit, M. Wijtmans, C. de Graaf, H. F. Vischer, R. Leurs, Pharmacological modulation of chemokine receptor function. *Br. J. Pharmacol.* **165**, 1617–1643 (2012).
14. M. P. Crump, J. H. Gong, P. Loetscher, K. Rajarathnam, A. Amara, F. Arenzana-Seisdedos, J. L. Virelizier, M. Baggiolini, B. D. Sykes, I. Clark-Lewis, Solution structure and basis for functional activity of stromal cell-derived factor-1; dissociation of CXCR4 activation from binding and inhibition of HIV-1. *EMBO J.* **16**, 6996–7007 (1997).
15. C. Blanpain, B. J. Doranz, A. Bondue, C. Govaerts, A. De Leener, G. Vassart, R. W. Doms, A. Proudfoot, M. Parmentier, The core domain of chemokines binds CCR5 extracellular domains while their amino terminus interacts with the transmembrane helix bundle. *J. Biol. Chem.* **278**, 5179–5187 (2003).
16. I. Kufareva, M. Gustavsson, Y. Zheng, B. S. Stephens, T. M. Handel, What do structures tell us about chemokine receptor function and antagonism? *Annu. Rev. Biophys.* **46**, 175–198 (2017).
17. L. Qin, I. Kufareva, L. G. Holden, C. Wang, Y. Zheng, C. Zhao, G. Fenalti, H. Wu, G. W. Han, V. Cherezov, R. Abagyan, R. C. Stevens, T. M. Handel, Crystal structure of the chemokine receptor CXCR4 in complex with a viral chemokine. *Science* **347**, 1117–1122 (2015).
18. J. S. Burg, J. R. Ingram, A. J. Venkatakrishnan, K. M. Jude, A. Dukkipati, E. N. Feinberg, A. Angelini, D. Waghray, R. O. Dror, H. L. Ploegh, K. C. Garcia, Structural biology. Structural basis for chemokine recognition and activation of a viral G protein–coupled receptor. *Science* **347**, 1113–1117 (2015).
19. Y. Zheng, G. W. Han, R. Abagyan, B. Wu, R. C. Stevens, V. Cherezov, I. Kufareva, T. M. Handel, Structure of CC chemokine receptor 5 with a potent chemokine antagonist reveals mechanisms of chemokine recognition and molecular mimicry by HIV. *Immunity* **46**, 1005–1017.e5 (2017).
20. J. J. Ziarek, A. B. Kleist, N. London, B. Raveh, N. Montpas, J. Bonneterre, G. St-Onge, C. J. DiCosmo-Ponticello, C. A. Koplinski, I. Roy, B. Stephens, S. Thelen, C. T. Veldkamp, F. D. Coffman, M. C. Cohen, M. B. Dwinell, M. Thelen, F. C. Peterson, N. Heveker, B. F. Volkman, Structural basis for chemokine recognition by a G protein–coupled receptor and implications for receptor activation. *Sci. Signal.* **10**, eaah5756 (2017).
21. Y. Kofuku, C. Yoshiura, T. Ueda, H. Terasawa, T. Hirai, S. Tominaga, M. Hirose, Y. Maeda, H. Takahashi, Y. Terashima, K. Matsushima, I. Shimada, Structural basis of the interaction between chemokine stromal cell-derived factor-1/CXCL12 and its G-protein-coupled receptor CXCR4. *J. Biol. Chem.* **284**, 35240–35250 (2009).
22. M. J. Walters, K. Ebsworth, R. D. Berahovich, M. E. Penfold, S.-C. Liu, R. Al Omran, M. Kioi, S. B. Chernikova, D. Tseng, E. E. Mulkearns-Hubert, M. Sinyuk, R. M. Ransohoff, J. D. Lathia, J. Karamchandani, H. E. Kohrt, P. Zhang, J. P. Powers, J. C. Jaen, T. J. Schall, M. Merchant, L. Recht, J. M. Brown, Inhibition of CXCR7 extends survival following irradiation of brain tumours in mice and rats. *Br. J. Cancer* **110**, 1179–1188 (2014).
23. X. Chen, P. Fan, M. M. Gleason, J. C. Jaen, L. Li, J. P. McMahon, J. Powers, Y. Zeng, and P. Zhang, *Modulators of CXCR7*, U.S. Patent number US8288373B2 (2010).
24. A. J. Zweemer, I. Nederpelt, H. Vrieling, S. Hafith, M. L. Doornbos, H. de Vries, J. Abt, R. Gross, D. Stamos, J. Saunders, M. J. Smit, A. P. Ijzerman, L. H. Heitman, Multiple binding sites for small-molecule antagonists at the CC chemokine receptor 2. *Mol. Pharmacol.* **84**, 551–561 (2013).
25. B. Vega, L. M. Muñoz, B. L. Holgado, P. Lucas, J. M. Rodríguez-Frade, A. Calle, J. L. Rodríguez-Fernández, L. M. Lechuga, J. F. Rodríguez, R. Gutiérrez-Gallego, M. Mellado, Technical advance: Surface plasmon resonance-based analysis of CXCL12 binding using immobilized lentiviral particles. *J. Leukoc. Biol.* **90**, 399–408 (2011).
26. D. P. Dyer, C. L. Salanga, B. F. Volkman, T. Kawamura, T. M. Handel, The dependence of chemokine–glycosaminoglycan interactions on chemokine oligomerization. *Glycobiology* **26**, 312–326 (2016).
27. M. Gustavsson, Y. Zheng, T. M. Handel, Production of chemokine/chemokine receptor complexes for structural biophysical studies. *Methods Enzymol.* **570**, 233–260 (2016).
28. T. Kawamura, B. Stephens, L. Qin, X. Yin, M. R. Dores, T. H. Smith, N. Grimsey, R. Abagyan, J. Trejo, I. Kufareva, M. M. Fuster, C. L. Salanga, T. M. Handel, A general method for site specific fluorescent labeling of recombinant chemokines. *PLOS ONE* **9**, e81454 (2014).
29. A. Manglik, B. Kobilka, The role of protein dynamics in GPCR function: Insights from the β2AR and rhodopsin. *Curr. Opin. Cell Biol.* **27**, 136–143 (2014).
30. B. T. DeVree, J. P. Mahoney, G. A. Vélez-Ruiz, S. G. Rasmussen, A. J. Kuszak, E. Edwald, J.-J. Fung, A. Manglik, M. Masureel, Y. Du, R. A. Matt, E. Pardon, J. Steyaert, B. K. Kobilka, R. K. Sunahara, Allosteric coupling from G protein to the agonist-binding pocket in GPCRs. *Nature* **535**, 182–186 (2016).
31. M. Castro, V. O. Nikolaev, D. Palm, M. J. Lohse, J.-P. Vilardaga, Turn-on switch in parathyroid hormone receptor by a two-step parathyroid hormone binding mechanism. *Proc. Natl. Acad. Sci. U.S.A.* **102**, 16084–16089 (2005).
32. A. I. Alexandrov, M. Mileni, E. Y. Chien, M. A. Hanson, R. C. Stevens, Microscale fluorescent thermal stability assay for membrane proteins. *Structure* **16**, 351–359 (2008).
33. M. S. Hanes, C. L. Salanga, A. B. Chowdry, I. Comerford, S. R. McColl, I. Kufareva, T. M. Handel, Dual targeting of the chemokine receptors CXCR4 and ACKR3 with novel engineered chemokines. *J. Biol. Chem.* **290**, 22385–22397 (2015).
34. B. Benredjem, M. Girard, D. Rhainds, G. St-Onge, N. Heveker, Mutational analysis of atypical chemokine receptor 3 (ACKR3/CXCR7) interaction with its chemokine ligands CXCL11 and CXCL12. *J. Biol. Chem.* **292**, 31–42 (2017).
35. M. Szpakowska, A. M. Nevins, M. Meyrath, D. Rhainds, T. D'huys, F. Guité-Vinet, N. Dupuis, P.-A. Gauthier, M. Counson, A. Kleist, G. St-Onge, J. Hanson, D. Schols, B. F. Volkman, N. Heveker, A. Chevigné, Different contributions of chemokine N-terminal features attest to a different ligand binding mode and a bias towards activation of ACKR3/CXCR7 compared with CXCR4 and CXCR3. *Br. J. Pharmacol.* **175**, 1419–1438 (2018).

36. Z. Rankovic, T. F. Brust, L. M. Bohn, Biased agonism: An emerging paradigm in GPCR drug discovery. *Bioorg. Med. Chem. Lett.* **26**, 241–250 (2016).
37. C. Klein Herenbrink, D. A. Sykes, P. Donthamsetti, M. Canals, T. Coudrat, J. Shonberg, P. J. Scammells, B. Capuano, P. M. Sexton, S. J. Charlton, J. A. Javitch, A. Christopoulos, J. R. Lane, The role of kinetic context in apparent biased agonism at GPCRs. *Nat. Commun.* **7**, 10842 (2016).
38. N. Montpas, G. St-Onge, N. Nama, D. Rhainds, B. Benredjem, M. Girard, G. Hickson, V. Pons, N. Heveker, Ligand-specific conformational transitions and intracellular transport are required for atypical chemokine receptor 3-mediated chemokine scavenging. *J. Biol. Chem.* **293**, 893–905 (2018).
39. K. Jarnagin, D. Grunberger, M. Mulkins, B. Wong, S. Hemmerich, C. Paavola, A. Bloom, S. Bhakta, F. Diehl, R. Freedman, D. McCarley, I. Polsky, A. Ping-Tsou, A. Kosaka, T. M. Handel, Identification of surface residues of the monocyte chemotactic protein 1 that affect signaling through the receptor CCR2. *Biochemistry* **38**, 16167–16177 (1999).
40. G. A. McQuibban, G. S. Butler, J.-H. Gong, L. Bendall, C. Power, I. Clark-Lewis, C. M. Overall, Matrix metalloproteinase activity inactivates the CXC chemokine stromal cell-derived factor-1. *J. Biol. Chem.* **276**, 43503–43508 (2001).
41. M. P. Wescott, I. Kufareva, C. Paes, J. R. Goodman, Y. Thaker, B. A. Puffer, E. Berdougo, J. B. Rucker, T. M. Handel, B. J. Doranz, Signal transmission through the CXC chemokine receptor 4 (CXCR4) transmembrane helices. *Proc. Natl. Acad. Sci. U.S.A.* **113**, 9928–9933 (2016).
42. J. Liu, S. Louie, W. Hsu, K. M. Yu, H. B. Nicholas Jr., G. L. Rosenquist, Tyrosine sulfation is prevalent in human chemokine receptors important in lung disease. *Am. J. Respir. Cell Mol. Biol.* **38**, 738–743 (2008).
43. J. P. Ludeman, M. J. Stone, The structural role of receptor tyrosine sulfation in chemokine recognition. *Br. J. Pharmacol.* **171**, 1167–1179 (2014).
44. N. L. Coggins, D. Trakimas, S. L. Chang, A. Ehrlich, P. Ray, K. E. Luker, J. J. Linderman, G. D. Luker, CXCR7 controls competition for recruitment of β-arrestin 2 in cells expressing both CXCR4 and CXCR7. *PLOS ONE* **9**, e98328 (2014).
45. J. Chiu, D. Tillett, I. W. Dawes, P. E. March, Site-directed, ligase-independent mutagenesis (SLIM) for highly efficient mutagenesis of plasmids greater than 8kb. *J. Microbiol. Methods* **73**, 195–198 (2008).
46. S. J. Allen, D. J. Hamel, T. M. Handel, A rapid and efficient way to obtain modified chemokines for functional and biophysical studies. *Cytokine* **55**, 168–173 (2011).
47. F. Hoffmann, W. Müller, D. Schütz, M. E. Penfold, Y. H. Wong, S. Schulz, R. Stumm, Rapid uptake and degradation of CXCL12 depend on CXCR7 carboxyl-terminal serine/threonine residues. *J. Biol. Chem.* **287**, 28362–28377 (2012).
48. M. Wijtmans, D. Maussang, F. Sirci, D. J. Scholten, M. Canals, A. Mujić-Delić, M. Chong, K. L. S. Chatalic, H. Custers, E. Janssen, C. de Graaf, M. J. Smit, I. J. P. de Esch, R. Leurs, Synthesis, modeling and functional activity of substituted styrene-amides as small-molecule CXCR7 agonists. *Eur. J. Med. Chem.* **51**, 184–192 (2012).
49. M. Canals, D. J. Scholten, S. de Munnik, M. K. L. Han, M. J. Smit, R. Leurs, Ubiquitination of CXCR7 controls receptor trafficking. *PLOS ONE* **7**, e34192 (2012).
50. B. A. Zabel, Y. Wang, S. Lewén, R. D. Berahovich, M. E. T. Penfold, P. Zhang, J. Powers, B. C. Summers, Z. Miao, B. Zhao, A. Jalili, A. Janowska-Wieczorek, J. C. Jaen, T. J. Schall, Elucidation of CXCR7-mediated signaling events and inhibition of CXCR4-mediated tumor cell transendothelial migration by CXCR7 ligands. *J. Immunol.* **183**, 3204–3211 (2009).
51. K. Balabanian, B. Lagane, S. Infantino, K. Y. C. Chow, J. Harriague, B. Moepps, F. Arenzana-Seisdedos, M. Thelen, F. Bachelerie, The chemokine SDF-1/CXCL12 binds to and signals through the orphan receptor RDC1 in T lymphocytes. *J. Biol. Chem.* **280**, 35760–35766 (2005).

Acknowledgments: We thank C. Salanga and B. Stephens for providing purified CXCL11 and CXCL12 protein, ChemoCentryx for the small-molecule compounds CCX662 and CCX777, and N. Heveker (Université de Montréal) for providing vectors for BRET experiments. **Funding:** This work was supported by grants from the NIH to T.M.H. (U01 GM094612, R21 AI121918, R01 GM117424, and R01 AI118985). M.G. was supported by a Robertson Foundation/Cancer Research Institute Irvington Postdoctoral Fellowship. **Author contributions:** D.P.D. and C.Z. designed, performed, and analyzed SPR experiments. M.G. designed and performed all other experiments, analyzed results, and wrote the paper. T.M.H. supervised the study, analyzed results, and wrote the paper. **Competing interests:** The authors declare that they have no competing interests. **Data and materials availability:** All data needed to evaluate the conclusions in the paper are present in the paper or the Supplementary Materials.

Submitted 13 December 2018
Accepted 14 August 2019
Published 10 September 2019
10.1126/scisignal.aaw3657

Citation: M. Gustavsson, D. P. Dyer, C. Zhao, T. M. Handel, Kinetics of CXCL12 binding to atypical chemokine receptor 3 reveal a role for the receptor N terminus in chemokine binding. *Sci. Signal.* **12**, eaaw3657 (2019).

Science Signaling

Kinetics of CXCL12 binding to atypical chemokine receptor 3 reveal a role for the receptor N terminus in chemokine binding

Martin Gustavsson, Douglas P. Dyer, Chunxia Zhao and Tracy M. Handel

Sci. Signal. **12** (598), eaaw3657.
DOI: 10.1126/scisignal.aaw3657

ACKR3 holds with a hug

Ligand-receptor interactions transduce signals intracellularly that induce cellular responses to the ligand. For the atypical chemokine receptor ACKR3, however, it instead binds and sequesters its ligands (chemokines) that it shares with other chemokine receptors, thereby limiting the amount of chemokine available to activate intracellular signaling. Gustavsson *et al.* discovered the role of the N terminus of ACKR3 in controlling its interaction with the chemokine CXCL12. Binding of the chemokine to the receptor was mediated through its N-terminal region as expected; however, the N terminus of ACKR3 then wrapped around regions of the chemokine to hold it more tightly. These findings have broad implications for understanding chemokine ligand-receptor interactions as well as both chemokine-specific cell biology and drug design.